# Boosting the activity of non-platinum group metal electrocatalyst for the reduction of oxygen via dual-ligated atomically dispersed precursors immobilized on carbon supports

Yu Zhou <sup>a, b,‡</sup> Talha Al-Zoubi <sup>a,‡</sup> Yanling Ma, <sup>a</sup> Haw-Wen Hsiao, <sup>c</sup> Cheng Zhang, <sup>a</sup>

Chengjun Sun, <sup>d</sup> Jian-Min Zuo <sup>c</sup> and Hong Yang <sup>a,\*</sup>

<sup>a</sup> Department of Chemical and Biomolecular Engineering, University of Illinois at Urbana-Champaign, 600 South Mathews Avenue, Urbana, IL 61801, USA

<sup>b</sup> State Key Laboratory of Chemical Engineering, Tianjin Key Laboratory of Membrane Science & Desalination Technology, School of Chemical Engineering and Technology, Tianjin University, Tianjin, 300350, China

<sup>c</sup> Department of Materials Science and Engineering, University of Illinois at Urbana-Champaign, 1304 W. Green Street, Urbana, Illinois 61801, USA

<sup>d</sup> X-ray Science Division, Argonne National Laboratory, 9700 South Cass Avenue, Argonne,
Illinois 60439, USA

\* Address correspondence to hy66@illinois.edu

‡: These authors contributed equally

**ABSTRACT** 

This paper describes the use of both atomically dispersed precursors (ADPs) and conductive

carbon dispersion towards the synthesis of iron-based single atom electrocatalysts for the

oxygen reduction reaction (ORR). For non-platinum group metal (non-PGM) catalysts, single

iron, cobalt or manganese atoms coordinated with nitrogen are the most active structures

towards the ORR. Achieving a high density of active sites made of single atoms is still

challenging, requiring careful controls of pyrolysis to reduce the sintering of metal active sites.

Herewith, we present a new strategy to synthesize iron-based single atom ORR electrocatalysts

using a two-pronged approach. We first designed a dual-ligated metal organic framework

(MOF) precursor. This MOF was then immobilized onto Ketjen black carbon that serves as a

conductive dispersion medium for creating the highly dispersed single atom sites. We

demonstrate a near complete dispersion of the iron sites without obvious formation of

nanoparticles. The activity of the resulting electrocatalyst exhibited an onset potential of 0.96

V and a half-wave potential of 0.84 V vs. reversible hydrogen electrode (RHE).

Keywords: dual-ligated, atomically dispersed, immobilized, non-platinum group metal, single

atom, oxygen reduction reaction

2

#### 1. Introduction

The development of new energy generation and utilization technology is important to move away from fossil fuel-based processes. A key driver is the use of renewable fuels generated from sustainable sources (e.g., wind and solar) for energy applications, such as transportation. In this context, hydrogen-powered polymer electrolyte membrane fuel cell (PEMFC) is a promising technology. The large-scale commercialization of PEMFCs for transportation applications however necessitates the development of highly active, low cost electrocatalysts for the oxygen reduction reaction (ORR) [1-10]. A key current research approach is to use low- or non-platinum group metal (PGM) electrocatalysts to make membrane electrodes for PEMFCs. Among them, nitrogen-coordinated iron (Fe), cobalt (Co), and manganese (Mn) based single atoms in carbon matrices are the most promising non-PGM electrocatalysts [11-20]. Synthesis procedure for these materials could have a critical impact on the final structures and chemical properties that govern catalytic performance. For high current density PEMFCs that are necessary for the heavy-duty vehicles, increasing the active sites of the electrocatalysts is important to achieve the performance targets.

Different methods have been developed for making single Fe and Co atom ORR electrocatalysts. Heteroatom-containing polymers and metal organic frameworks (MOFs) are often used as atomically dispersed precursors (ADPs) in the synthesis of these kinds of electrocatalysts [16, 20-33]. There are several advantages in using the ADPs for making the electrocatalysts. Firstly, the ADPs inherently contain the required elements (C, N and metal). Secondly, the method allows for the spatial confinement of metal single atoms. Thirdly, the resulting porous structures may further facilitate a high level of dispersion of the active elements throughout the lattice. The ADPs need to be treated at high temperatures to generate porous carbon structures with highly dispersed metal-nitrogen moieties, which are essential for high activity. Avoiding the formation of metal nanoparticles, which have been shown to be less

active towards the ORR, is often necessary but often challenging because of the high temperature needed to convert the ADPs into active species through the pyrolysis [28, 34-36]. Studies have shown through elemental substitution in the precursor, reaction temperature could be optimized, resulting in the formation of single atom active structures at a reduced temperature which further limited the formation of nanoparticles [16]. Currently, the zeolitic imidazolate framework (ZIF-8) is one of the most commonly used precursors in the synthesis of highly active electrocatalysts for the ORR, though other MOFs have also been used as the ADPs [18, 32, 37, 38].

In this study, we developed a strategy to synthesize single Fe atom ORR electrocatalysts. On the selection of ADPs for the preparation of non-PGM ORR electrocatalysts, we used a dual-ligated MOF with 1,4-diazabicyclo[2.2.2]octane (DABCO) as the N-containing ligand and terephthalic acid (TPA) as the organic linkers. In this case, the oxygen-containing ligand (i.e., TPA) coordinates to the metal atoms in a two-dimensional plane, while the nitrogencontaining ligand (i.e., DABCO) serves as the other linker to form the three-dimensional framework [39]. Unlike ZIF-8 or other single-ligand MOFs, the use of a secondary ligand helps to increase the control of interatomic distances between the metal nodes, thus the new opportunity to optimize distances between Fe atoms within the MOFs [16, 23, 28, 40-44]. In addition, we immobilized ADPs onto conductive supports to further increase the Fe and N atomic dispersions. This immobilization step served to anchor and stabilize the single atom sites during pyrolysis [45]. Following this two-pronged design concept, we developed a highly active non-PGM electrocatalyst with uniformly dispersed single atom sites on carbon support. The obtained non-PGM ORR electrocatalysts exhibited an onset potential (E<sub>onset</sub>) of 0.96 V and a half-wave potential (E<sub>1/2</sub>) of 0.84 V (vs. RHE) in a 0.1 M perchloric acid (HClO<sub>4</sub>) electrolyte tested using a graphite rod as the counter electrode, which are among the most active non-PGM ORR electrocatalysts reported [13].

#### 2. Results and discussion

# 2.1 Preparation of the MOFs derived Fe-N-C electrocatalysts

**Fig. 1** illustrates the synthetic route for the preparation of Fe-based atomically dispersed non-PGM electrocatalysts. A Zn-Fe-DABCO-TPA MOF was synthesized from a mixture of DABCO (N-containing ligand), TPA, Zn(NO<sub>3</sub>)<sub>2</sub>, and Fe(NO<sub>3</sub>)<sub>3</sub>. The MOF precursor was then loaded onto Ketjen black carbon. Finally, a Fe-based non-PGM ORR electrocatalyst was prepared through the pyrolysis at a predetermined temperature in the range of 850 °C to 1,050 °C under an Ar atmosphere.

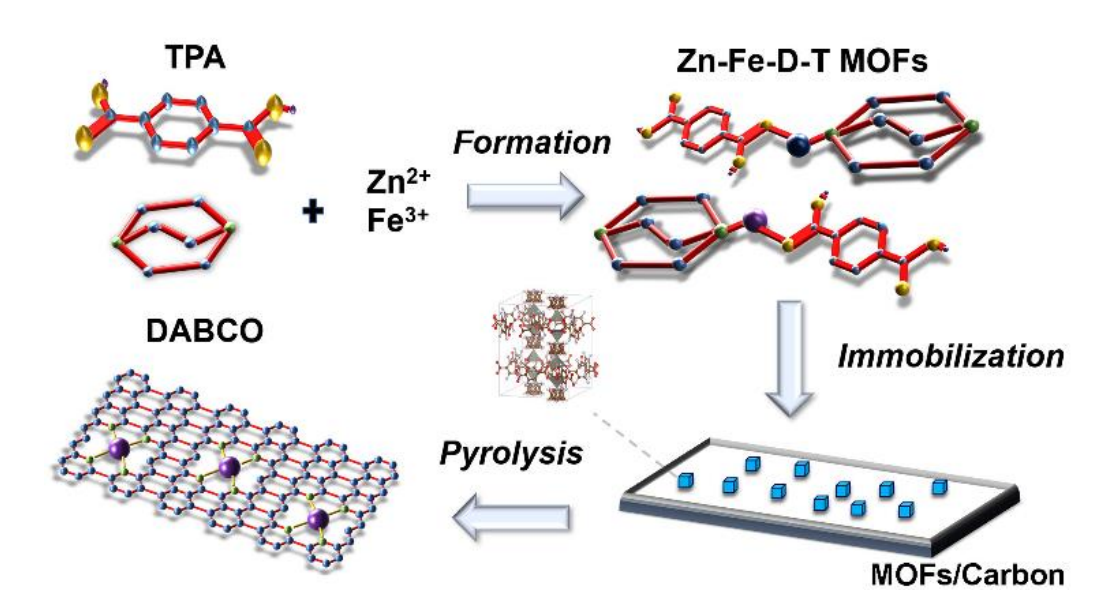


**Fig. 1.** Illustration of the synthesis route to the non-PGM electrocatalyst using dual-ligated MOF precursors immobilized on a conductive support.

# 2.2 Structure identifications of Fe–N–C electrocatalysts

The non-PGM electrocatalyst was made from a MOF precursor containing Fe as the active metal and exhibited faceted morphologies with the long edge length in the range of 1 to 2  $\mu$ m

(Fig. S1). The PXRD pattern shows the as-synthesized MOF precursor was highly crystalline (Fig. S2). Fig. 2a shows the TEM micrograph of the produced electrocatalysts which exhibit porous structures without any observable nanoparticles. The TEM study showed the high temperature pyrolysis did not lead to the formation of nanoparticles. In contrast, the control catalyst of Fe-D-T<sub>950</sub>, which was synthesized under similar conditions but without the use of a carbon support, consisted of a number of nanoparticles (Fig. S3). This observation suggests that the immobilization of ADPs onto the carbon support could help in anchoring the assynthesized MOFs and reduce the possibility of sintering though the interaction between the carbon support and MOF precursor. Such interactions effectively reduce the sintering of metal atoms during the pyrolysis step. Aberration-corrected annular dark-field (ADF) STEM study shows bright spots, which are indicated by the yellow arrow and correspond to single Fe atoms on carbon support (Fig. 2b) [16]. The final atomic Fe loadings in both Fe/C<sub>950</sub> and Fe-D-T<sub>950</sub> were determined using ICP-MS measurement and the results were summarized in Table S1. The metal loading for the  $Fe/C_{950}$  electrocatalyst was determined to be 0.72 wt.%. This value is lowered than those obtained using the procedure without the use of carbon dispersion media and likely resulted from the additional amount of conductive carbon used in this procedure.

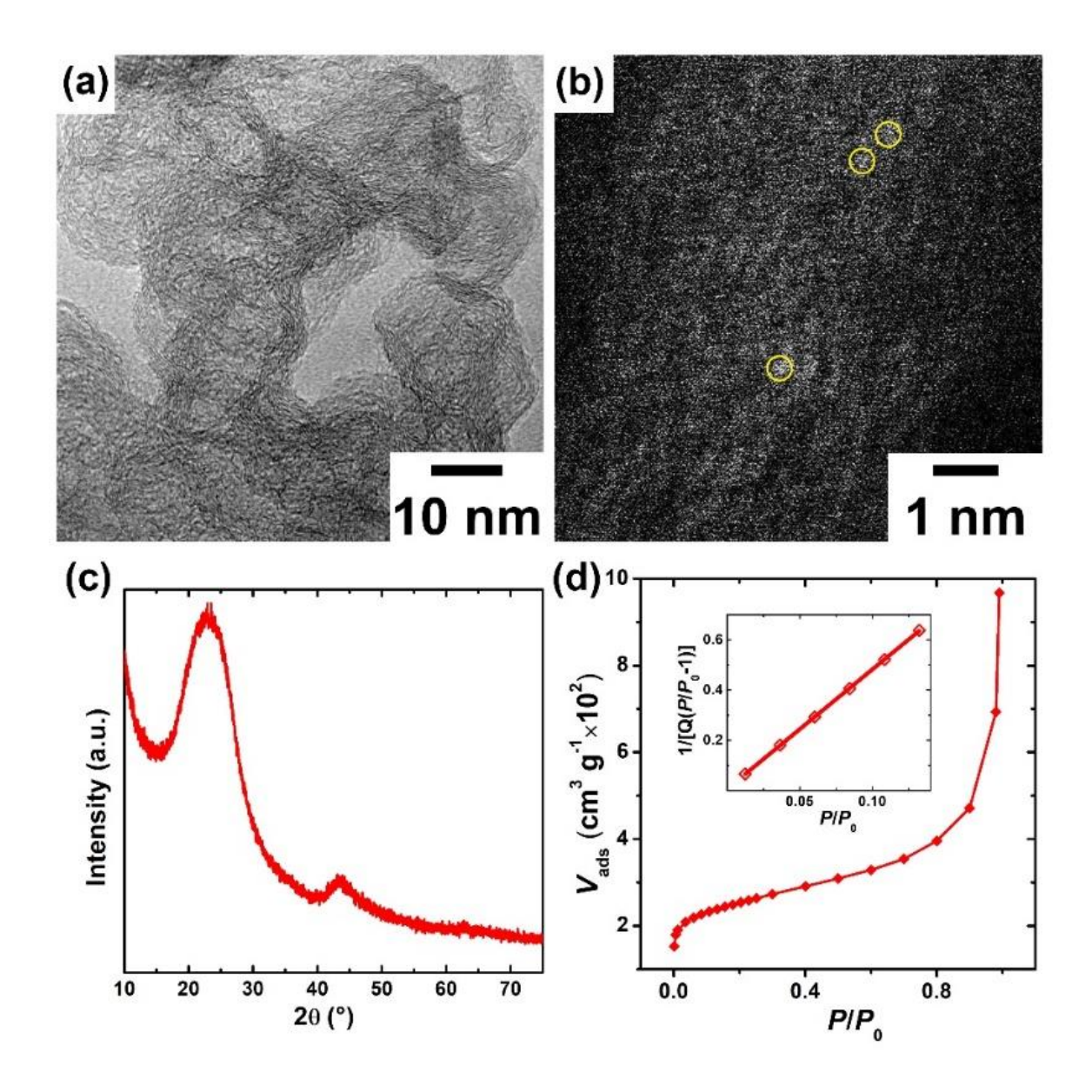


**Fig. 2.** (a) TEM micrograph, (b) ADF-STEM image, (c) PXRD pattern, and (d) N<sub>2</sub> isotherm analysis of the Fe/C<sub>950</sub> electrocatalyst, showing the dispersion of single atom moieties and the lack of iron-containing nanoparticles.

**Fig. 2c** shows the PXRD pattern of a typical Fe/C<sub>950</sub> catalyst, which exhibits two broad peaks centred at 22° and 43° 2θ, corresponding to graphitic carbon [38, 46]. The diffraction peaks are broad, indicating a large degree of disordering, which might be attributed to the N and Fe atoms incorporated in the amorphous carbon matrices. In the case of Fe-D-T<sub>950</sub>, in addition to the peaks attributed to graphitic carbon, diffractions from iron oxide (Fe<sub>2</sub>O<sub>3</sub>)

nanoparticles were observed (**Fig. S4**). These results agreed with those from the TEM study. In contrast, when a carbon dispersion medium was used, no metal or metal oxide nanoparticles were observed in the PXRD patterns (**Fig. S5**) or TEM micrographs (**Fig. S6**) at the pyrolysis temperature of 850 °C and 1,050 °C, respectively. The Brunauer-Emmet-Teller (BET) analysis exhibited a specific surface area of 912 m<sup>2</sup> g<sup>-1</sup> for the Fe/C<sub>950</sub> catalyst and 714 m<sup>2</sup> g<sup>-1</sup> for Fe-D-T<sub>950</sub> (**Fig. 2d**). The high specific surface area observed in Fe/C<sub>950</sub> could be attributed to the use of Ketjen black carbon as the dispersion media. The large specific surface area is preferred for the formation of single atom sites, and likely led to an increased density of active sites post-pyrolysis [47]. The convergent evidence shows that the Fe/C<sub>950</sub> catalyst is largely composed of Fe single atoms without nanoparticles.

# 2.3 Catalytic performance

ORR activities of the Fe/C electrocatalysts and the corresponding controls were evaluated in a 0.1-M HClO<sub>4</sub> electrolyte using the RDE technique. Catalyst inks were prepared using a Nafion solution and deposited onto the surface of a glassy carbon electrode to achieve a loading amount of ca. 1.0 mg cm<sup>-2</sup>. Samples made at three different temperatures (850 °C, 950 °C, and 1050 °C) were examined to determine their activities [16, 35, 48]. **Fig. 3a** shows the linear sweep voltammograms for all three non-PGM Fe/C<sub>T</sub> electrocatalysts. Our results indicate there exists an optimal pyrolysis temperature of 950 °C, under which the Fe/C<sub>950</sub> electrocatalyst had both the highest E<sub>onset</sub> and the E<sub>1/2</sub> among the non-PGM samples (**Fig. 3b**). The polarization curve data shows the Fe/C<sub>950</sub> exhibited a high E<sub>onset</sub> of 0.96 V and an E<sub>1/2</sub> of 0.84 V (vs. RHE). Both values were higher than those measured for the reference Pt/C under the same RDE testing conditions using a graphite rod as the counter electrode. The Koutecky-Levich analysis was performed at the rotation rates between 400 rpm and 2500 rpm to analyse the charge transfer

of the reaction (**Fig. 3c**) [49]. The results show that the Fe/C<sub>950</sub> electrocatalyst underwent a four-electron pathway in the ORR (**Fig. 3d**).

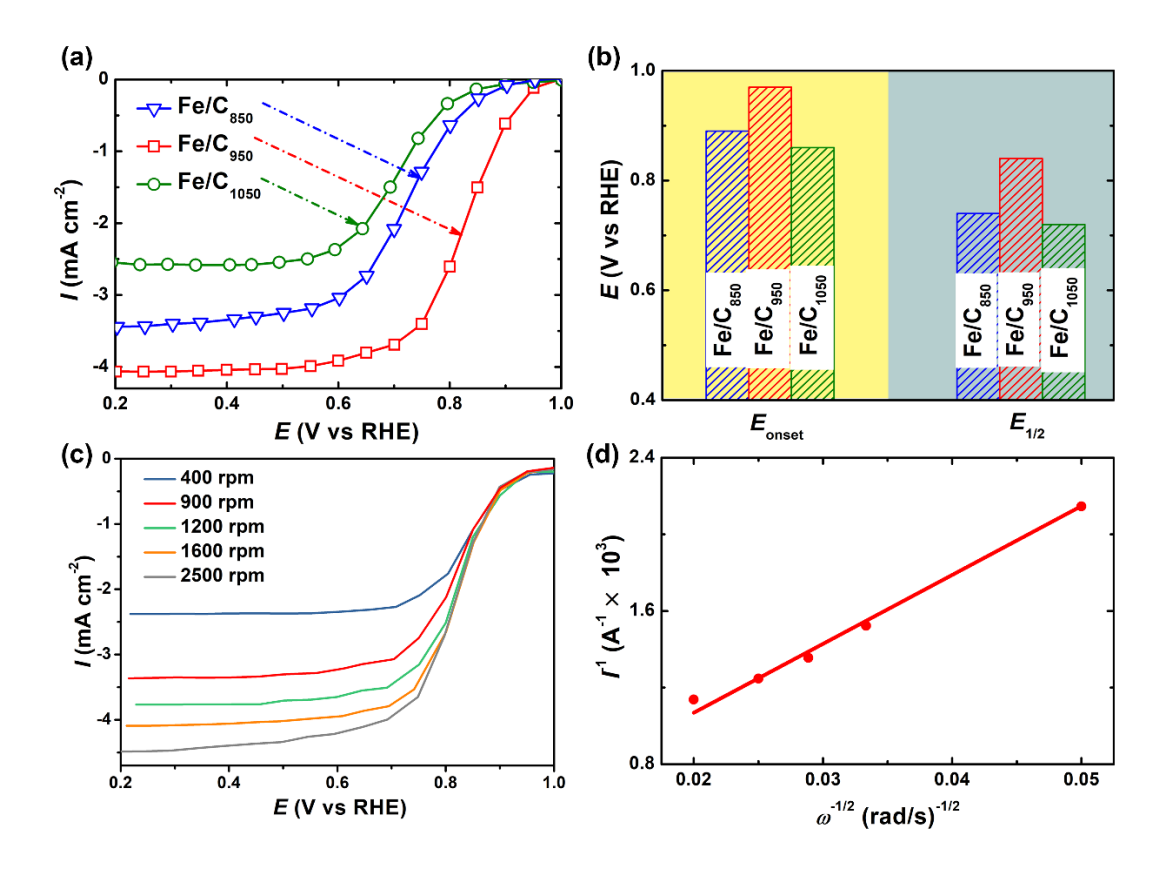


**Fig. 3.** (a) Linear sweep voltammograms obtained at the rotation rate of 900 rpm, (b) the corresponding  $E_{onset}$  and  $E_{1/2}$ , (c) Koutecky-Levich measurement and (d) analysis of the Fe/C<sub>950</sub> electrocatalyst. The Fe/C<sub>850</sub> and Fe/C<sub>1050</sub> are included for comparison. Test conditions were as the following: O<sub>2</sub>-saturated 0.1 M HClO<sub>4</sub> solution; catalyst loading, 1 mg cm<sup>-2</sup>.

Linear sweep voltammograms were performed using multiple control catalysts (**Fig. S7**) to understand the contributing structural factors of the high ORR activity of Fe/C<sub>950</sub> catalyst. To examine the effect of dual ligands, we tested various MOF-derived controls obtained after the pyrolysis at 950 °C (i.e., Fe-D<sub>950</sub>, Fe-T<sub>950</sub> and Fe-D-T<sub>950</sub>). The performances of Co-based electrocatalysts (i.e. Co/C<sub>950</sub> and Co<sub>950</sub> for the samples with and without immobilization on conductive carbon, respectively) were also examined. Our results indicate the Fe-D-T<sub>950</sub> has a

better ORR activity than the other two controls, with a E<sub>1/2</sub> of 0.77 V in 0.1M HClO<sub>4</sub>, but a worse activity than the Fe/C<sub>950</sub> (**Fig. 4a**). Compared to dual ligated precursors, the controls obtained using only one ligand precursor showed almost no active towards ORR. By introducing dual ligands, the three-dimension structures were formed with highly dispersion of metal atoms[39, 50]. The distance between neighboring metal atoms could be tuned by the feeding ratio of different ligands [38]. The used of immobilizing carbon further improved the dispersion of metal atoms, resulting in even higher ORR activities, likely due to the Fe single atom species produced during the heating treatment.

It is noteworthy that the dual-ligand and immobilization strategies are also effective for making the Co-containing non-PGM electrocatalysts, which exhibited a similar catalytic activity-processing condition trend. The half-wave potential of Co/C<sub>950</sub> for ORR increased significantly by 100 mV in 0.1M HClO<sub>4</sub> for the sample using the immobilization procedure (**Fig. 4b**).

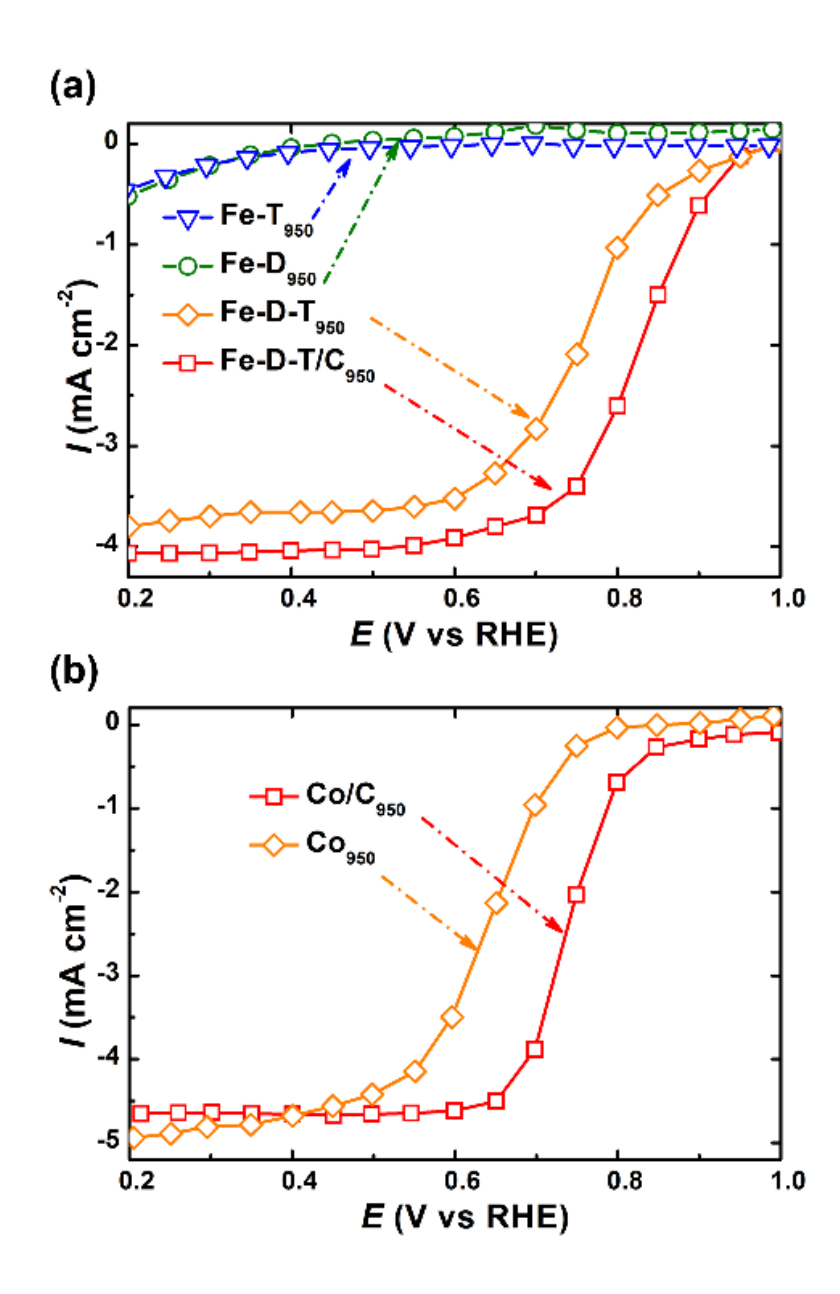


**Fig. 4.** Linear sweep voltammograms of the control electrocatalysts tested using the RDE method: (a) Fe-T<sub>950</sub>, Fe-D<sub>950</sub>, Fe-D-T<sub>950</sub> and Fe-D-T/C<sub>950</sub> (or Fe/C<sub>950</sub>). (b) Co/C<sub>950</sub> and Co<sub>950</sub>. Test conditions were as the following: O<sub>2</sub>-saturated 0.1 M HClO<sub>4</sub> solution; catalyst loading, 1 mg cm<sup>-2</sup>, rotation rate of 900 rpm.

# 2.4 XAS and XPS characterizations

The performance of non-PGM ORR electrocatalysts is often related to the local structures of the active sites. We thus examined the effects of the carbon structure, nitrogen binding,

catalyst porosity and morphology on the activity of these electrocatalysts. X-ray adsorption near-edge spectroscopy (XANES) was used to investigate the chemical environment of the Fe atoms by evaluating the oxidation states of each catalyst. Fe/C<sub>950</sub> and Fe-D-T<sub>950</sub> were investigated to elucidate the impact of the carbon dispersion on the formation of single atom Fe. Fig. 5a show the XANES of Fe K-edge region for both the Fe/C<sub>950</sub> and Fe-D-T<sub>950</sub> electrocatalysts, and the corresponding Fe foil as the reference. The results indicate that the overall oxidation state of the Fe single atoms in both Fe-containing electrocatalysts exhibited a higher edge than that in the Fe foil. The extended X-ray absorption fine structure (EXAFS) spectroscopy shows the structural difference between the Fe/C<sub>950</sub> and Fe-D-T<sub>950</sub> electrocatalysts (Fig. 5b). While the Fe-N bond with a length of 1.5 Å was detected for the corresponding first shells in both Fe-D-T<sub>950</sub> and Fe/C<sub>950</sub> electrocatalysts, the peak around 2.5 Å, which is derived from iron cation, such as Fe<sub>2</sub>O<sub>3</sub>[35], was observed for the control of the Fe-D-T<sub>950</sub> electrocatalyst, consistent with the XRD analysis. The XAS data thus help to confirm the single Fe atoms in Fe/C<sub>950</sub> electrocatalyst, without the obvious formation of Fe nanoparticles. The EXAFS data indicate the presence of the Fe-N bonds in the Fe/C<sub>950</sub> electrocatalysts.

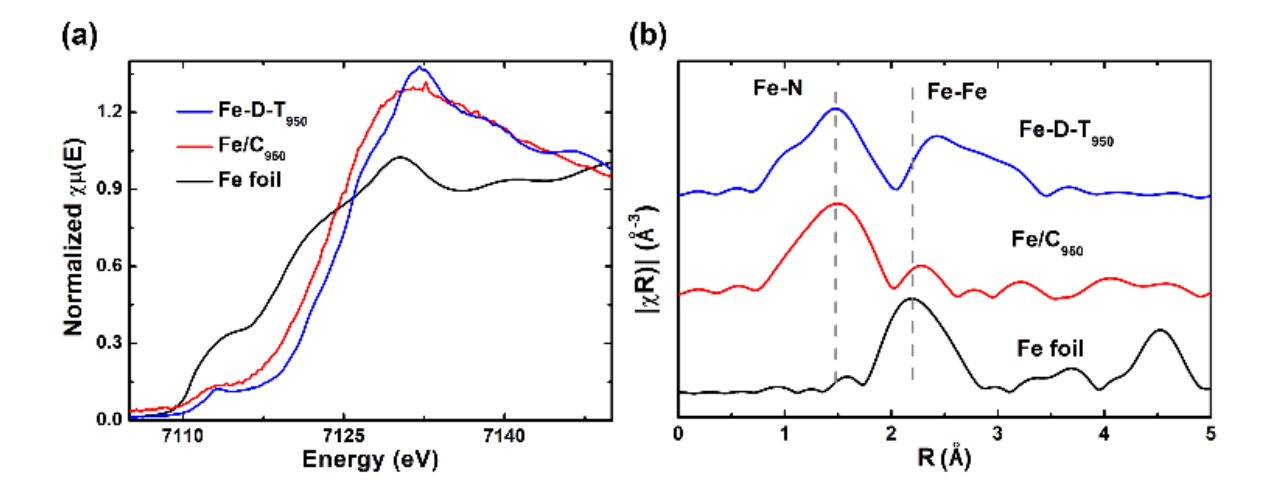
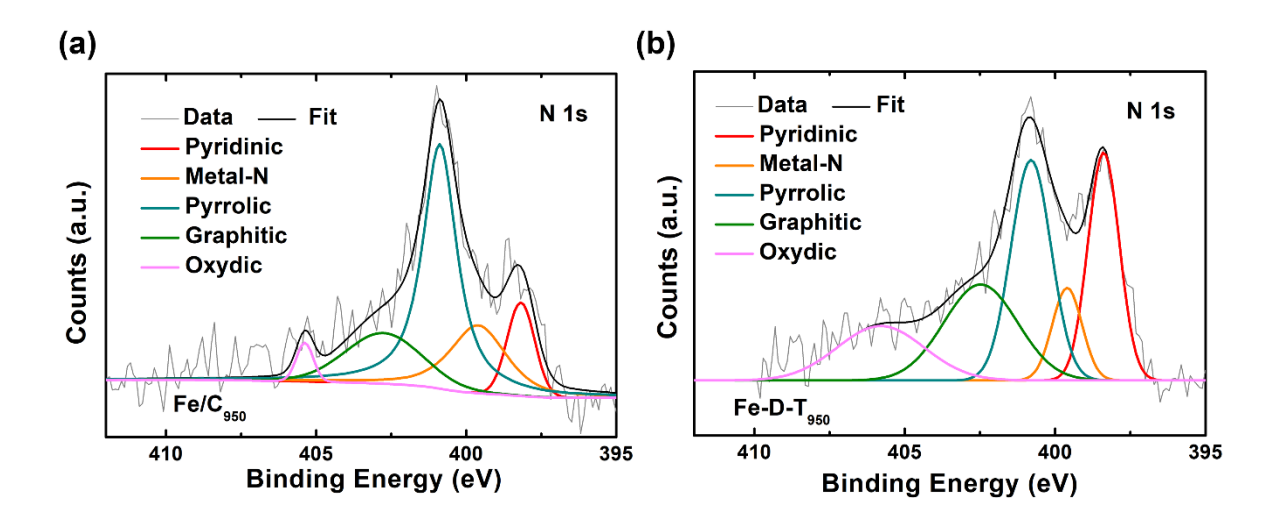


Fig. 5. (a) XANES and (b) EXAFS of Fe K-edge for Fe/C<sub>950</sub> and Fe-D-T<sub>950</sub> electrocatalysts.

X-ray photoelectron spectroscopy was used to examine the surface structures of these two electrocatalysts in order to elucidate the binding structures of Fe (**Fig. 6** and **Table S2**)[16, 51, 52]. The XPS for the N 1s region shows both the Fe/C<sub>950</sub> and Fe-D-T<sub>950</sub> samples exhibit nitrogen peaks pertaining to the pyridinic and pyrrolic species. In addition, metal-N peaks were detected for both catalysts. Such nitrogen structures were attributed to the Fe atoms for the high activity observed in non-PGM electrocatalysts.[53] The presence of Fe-N peaks in both Fe/C<sub>950</sub> and Fe-D-T<sub>950</sub> electrocatalysts is indicative that the single Fe atomic moieties are strongly coordinated by nitrogen atoms.



**Fig. 6.** XPS spectra of N 1s regions for the (a) Fe/C<sub>950</sub> and (b) Fe-D-T<sub>950</sub> electrocatalysts, respectively.

#### 2.5 Raman characterizations

Graphitic structures in carbon often contribute to the ORR activity in the non-PGM electrocatalysts [34, 35]. We thus used Raman spectroscopy to investigate the defect ratio of the carbon structures in the optimal electrocatalyst (Fe/C<sub>950</sub>) and compare it with that of the control made without the use of carbon black (Fe-D-T<sub>950</sub>) (**Table S3**). Both the disorder-

induced D-band and the G-band were observed for the carbon in the Raman spectroscopy. Using the peak area ratios between these two bands, the relative graphitic nature of the carbon matrix can be analyzed in these non-PGM electrocatalysts (**Fig. 7**) [54-57]. Our results indicate that D/G ratio is 2.81 for the Fe/C<sub>950</sub> sample and 1.81 for the Fe<sub>950</sub>. A large D/G ratio is often an indicative of disordered graphitic structures, suggesting the Fe/C<sub>950</sub> electrocatalysts possess a high degree of disordered graphitic structures because of the presence of large amount of single iron atomic structures.

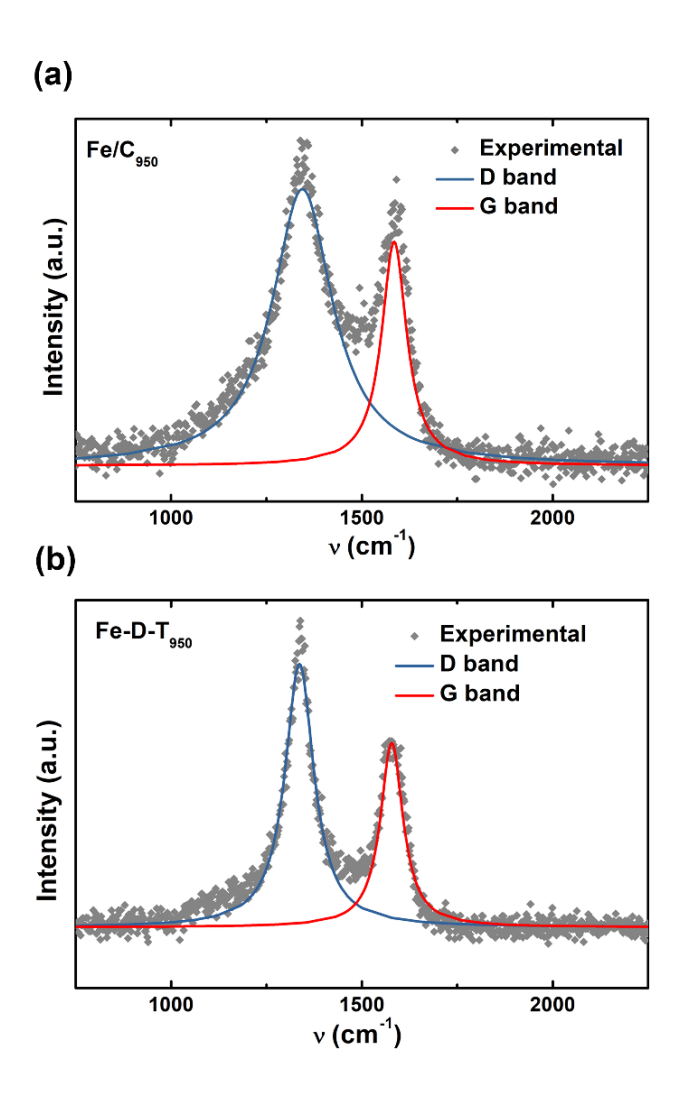


**Fig. 7.** Raman spectra for (a) Fe/C<sub>950</sub> and (b) Fe-D-T<sub>950</sub> depicting the D band and G band ratios.

#### 3. Conclusion

In summary, we developed a synthetic strategy of using dual-ligated MOF as the ADPs and conductive carbon dispersion as the immobilization media to generate atomically dispersed single Fe electrocatalysts for the ORR. The non-PGM electrocatalyst produced consists primarily single iron atom sites without nanoparticles and exhibits a high half-wave potential of 0.84 V vs. RHE. The approach developed in this study should be capable of producing catalysts with high single atom density and a useful design towards the preparation of high-performance non-PGM electrocatalysts.

# **Declaration of competing interest**

The authors declare no competing financial interest.

## **CRediT** authorship contribution statement

Yu Zhou: Conceptualization, Methodology, Writing - original draft, Writing - review & editing, Data curation, Validation, Formal analysis, Investigation. Talha Al-Zoubi: Conceptualization, Methodology, Data curation, Writing - review & editing. Yangling Ma: Data curation, Methodology. Haw-Wen Hsiao: Characterization. Cheng Zhang: Data curation, Writing - review & editing. Chengjun Sun: Characterization. Jian-Min Zuo: Characterization. Hong Yang: Supervision, Conceptualization, Investigation, Resources, Funding acquisition, Writing - review & editing.

## Acknowledgments

This work is supported in part by the Chinese-American Railway Transportation Joint Research Center at UIUC. Electron microscopy characterization was carried out at the Materials Research Laboratory at the University of Illinois. This research used resources of the Advanced Photon Source; an Office of Science User Facility operated for the U.S. Department of Energy (DOE) Office of Science by Argonne National Laboratory (DE-AC02-06CH11357). We extend our thanks to Dr. Richard T. Haasch and Dr. Kiran Subedi for their technical assistance, and to Dr. Andrew Gewirth for valuable discussions.

# Appendix A. Supplementary data

Supplementary data to this article can be found online.

#### References

- [1] X. Wan, X. Liu, Y. Li, R. Yu, L. Zheng, W. Yan, H. Wang, M. Xu, J. Shui, Fe–N–C electrocatalyst with dense active sites and efficient mass transport for high-performance proton exchange membrane fuel cells, Nat. Catal. 2 (2019) 259-268.
- [2] C.S. Gittleman, A. Kongkanand, D. Masten, W.B. Gu, Materials research and development focus areas for low cost automotive proton-exchange membrane fuel cells, Curr Opin Electrochem 18 (2019) 81-89.
- [3] Y. Shi, Z. Lyu, M. Zhao, R. Chen, Q.N. Nguyen, Y. Xia, Noble-metal nanocrystals with controlled shapes for catalytic and electrocatalytic applications, Chem. Rev. 121 (2020) 649-735.
- [4] P. Strasser, Catalysts by platonic design, Science 349 (2015) 379-380.
- [5] J. Wu, H. Yang, Platinum-based oxygen reduction electrocatalysts, Acc. Chem. Res. 46 (2013) 1848-1857.
- [6] Z. Peng, H. Yang, Designer platinum nanoparticles: control of shape, composition in alloy, nanostructure and electrocatalytic property, Nano Today 4 (2009) 143-164.
- [7] F.J. Zhu, J. Kim, K.C. Tsao, J.L. Zhang, H. Yang, Recent development in the preparation of nanoparticles as fuel cell catalysts, Curr. Opin. Chem. Eng. 8 (2015) 89-97.
- [8] Y.J. Kang, P.D. Yang, N.M. Markovic, V.R. Stamenkovic, Shaping electrocatalysis through tailored nanomaterials, Nano Today 11 (2016) 587-600.
- [9] Y. Ma, A.N. Kuhn, W. Gao, T. Al-Zoubi, H. Du, X. Pan, H. Yang, Strong electrostatic adsorption approach to the synthesis of sub-three nanometer intermetallic platinum–cobalt oxygen reduction catalysts, Nano Energy 79 (2021) 105465.
- [10] L. Chong, J. Wen, J. Kubal, F.G. Sen, J. Zou, J. Greeley, M. Chan, H. Barkholtz, W. Ding, D.-J. Liu, Ultralow-loading platinum-cobalt fuel cell catalysts derived from imidazolate frameworks, Science 362 (2018) 1276-1281.
- [11] M. Chen, Y. He, J.S. Spendelow, G. Wu, Atomically dispersed metal catalysts for oxygen reduction, ACS Energy Lett. 4 (2019) 1619-1633.
- [12] M. Shao, Q. Chang, J.-P. Dodelet, R. Chenitz, Recent advances in electrocatalysts for oxygen reduction reaction, Chem. Rev. 116 (2016) 3594-3657.
- [13] A.A. Gewirth, J.A. Varnell, A.M. DiAscro, Nonprecious metal catalysts for oxygen reduction in heterogeneous aqueous systems, Chem. Rev. 118 (2018) 2313-2339.

- [14] J. Wang, Z. Huang, W. Liu, C. Chang, H. Tang, Z. Li, W. Chen, C. Jia, T. Yao, S. Wei, Y. Wu, Y. Li, Design of N-coordinated dual-metal sites: a stable and active Pt-free catalyst for acidic oxygen reduction reaction, J. Am. Chem. Soc. 139 (2017) 17281-17284.
- [15] G. Wu, K.L. More, C.M. Johnston, P. Zelenay, High-performance electrocatalysts for oxygen reduction derived from polyaniline, iron, and cobalt, Science 332 (2011) 443-447.
- [16] T. Al-Zoubi, Y. Zhou, X. Yin, B. Janicek, C. Sun, C.E. Schulz, X. Zhang, A.A. Gewirth, P. Huang, P. Zelenay, H. Yang, Preparation of nonprecious metal electrocatalysts for the reduction of oxygen using a low-temperature sacrificial metal, J. Am. Chem. Soc. 142 (2020) 5477-5481.
- [17] X. Xie, C. He, B. Li, Y. He, D.A. Cullen, E.C. Wegener, A.J. Kropf, U. Martinez, Y. Cheng, M.H. Engelhard, M.E. Bowden, M. Song, T. Lemmon, X.S. Li, Z. Nie, J. Liu, D.J. Myers, P. Zelenay, G. Wang, G. Wu, V. Ramani, Y. Shao, Performance enhancement and degradation mechanism identification of a single-atom Co–N–C catalyst for proton exchange membrane fuel cells, Nat. Catal. 3 (2020) 1044-1054.
- [18] T. Al-Zoubi, W. Gao, C.E. Schulz, D. Luo, A.M. DiAscro, J. Wen, A.A. Gewirth, H. Yang, Effects of superparamagnetic iron nanoparticles on electrocatalysts for the reduction of oxygen, Inorg. Chem. 60 (2021) 4236-4242.
- [19] J. Li, M.T. Sougrati, A. Zitolo, J.M. Ablett, I.C. Oğuz, T. Mineva, I. Matanovic, P. Atanassov, Y. Huang, I. Zenyuk, A. Di Cicco, K. Kumar, L. Dubau, F. Maillard, G. Dražić, F. Jaouen, Identification of durable and non-durable FeNx sites in Fe–N–C materials for proton exchange membrane fuel cells, Nat. Catal. 4 (2021) 10-19.
- [20] X.F. Lu, B.Y. Xia, S.Q. Zang, X.W. Lou, Metal-Organic Frameworks Based Electrocatalysts for the Oxygen Reduction Reaction, Angew. Chem. Int. Ed. 59 (2020) 4634-4650.
- [21] H.M. Barkholtz, D.-J. Liu, Advancements in rationally designed PGM-free fuel cell catalysts derived from metal-organic frameworks, Mater. Horiz. 4 (2017) 20-37.
- [22] H. Zhang, H. Osgood, X. Xie, Y. Shao, G. Wu, Engineering nanostructures of PGM-free oxygen-reduction catalysts using metal-organic frameworks, Nano Energy 31 (2017) 331-350.
- [23] S. Ma, A. Goenaga Gabriel, V. Call Ann, D.J. Liu, Cobalt imidazolate framework as precursor for oxygen reduction reaction electrocatalysts, Chem. Eur. J. 17 (2011) 2063-2067.

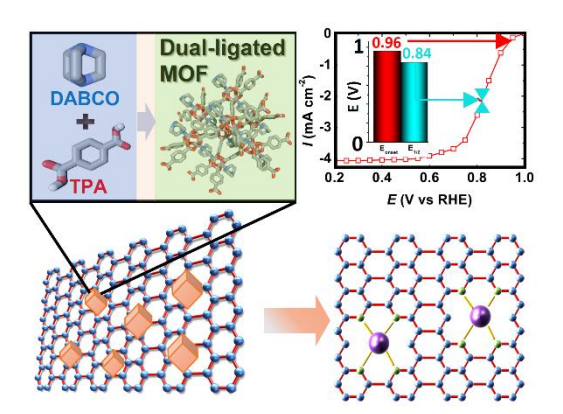
- [24] X. Wang, H. Zhang, H. Lin, S. Gupta, C. Wang, Z. Tao, H. Fu, T. Wang, J. Zheng, G. Wu, X. Li, Directly converting Fe-doped metal-organic frameworks into highly active and stable Fe-N-C catalysts for oxygen reduction in acid, Nano Energy 25 (2016) 110-119.
- [25] X. Wang, X. Fan, H. Lin, H. Fu, T. Wang, J. Zheng, X. Li, An efficient Co-N-C oxygen reduction catalyst with highly dispersed Co sites derived from a ZnCo bimetallic zeolitic imidazolate framework, RSC Adv. 6 (2016) 37965-37973.
- [26] H. Tang, S. Cai, S. Xie, Z. Wang, Y. Tong, M. Pan, X. Lu, Metal-organic-framework-derived dual metal- and nitrogen-doped carbon as efficient and robust oxygen reduction reaction catalysts for microbial fuel cells, Adv. Sci. 3 (2016) 1500265.
- [27] Z. Li, M. Shao, L. Zhou, Q. Yang, C. Zhang, M. Wei, D.G. Evans, X. Duan, Carbon-based electrocatalyst derived from bimetallic metal-organic framework arrays for high performance oxygen reduction, Nano Energy 25 (2016) 100-109.
- [28] V. Armel, S. Hindocha, F. Salles, S. Bennett, D. Jones, F. Jaouen, Structural descriptors of zeolitic-imidazolate frameworks are keys to the activity of Fe-N-C catalysts, J. Am. Chem. Soc. 139 (2017) 453-464.
- [29] T. Sun, L. Xu, D. Wang, Y. Li, Metal organic frameworks derived single atom catalysts for electrocatalytic energy conversion, Nano Res. 12 (2019) 2067–2080.
- [30] Y. He, S. Hwang, D.A. Cullen, M.A. Uddin, L. Langhorst, B. Li, S. Karakalos, A.J. Kropf, E.C. Wegener, J. Sokolowski, M. Chen, D. Myers, D. Su, K.L. More, G. Wang, S. Litster, G. Wu, Highly active atomically dispersed CoN<sub>4</sub> fuel cell cathode catalysts derived from surfactant-assisted MOFs: carbon-shell confinement strategy, Energ. Environ. Sci. 12 (2019) 250-260.
- [31] L. Li, J. He, Y. Wang, X. Lv, X. Gu, P. Dai, D. Liu, X. Zhao, Metal-organic frameworks: a promising platform for constructing non-noble electrocatalysts for the oxygen-reduction reaction, J. Mater. Chem. A 7 (2019) 1964-1988.
- [32] X.F. Lu, B.Y. Xia, S.-Q. Zang, X.W. Lou, Metal-organic frameworks based electrocatalysts for the oxygen reduction reaction, Angew. Chem. Int. Ed. 59 (2020) 4634-4650.
- [33] Q. Shi, S. Hwang, H. Yang, F. Ismail, D. Su, D. Higgins, G. Wu, Supported and coordinated single metal site electrocatalysts, Mater. Today 37 (2020) 93-111.
- [34] A. Zitolo, V. Goellner, V. Armel, M.T. Sougrati, T. Mineva, L. Stievano, E. Fonda, F. Jaouen, Identification of catalytic sites for oxygen reduction in iron- and nitrogen-doped graphene materials, Nat. Mater. 14 (2015) 937-942.

- [35] H. Zhang, S. Hwang, M. Wang, Z. Feng, S. Karakalos, L. Luo, Z. Qiao, X. Xie, C. Wang, D. Su, Y. Shao, G. Wu, Single atomic iron catalysts for oxygen reduction in acidic media: particle size control and thermal activation, J. Am. Chem. Soc. 139 (2017) 14143-14149.
- [36] H. Zhang, H.T. Chung, D.A. Cullen, S. Wagner, U.I. Kramm, K.L. More, P. Zelenay, G. Wu, High-performance fuel cell cathodes exclusively containing atomically dispersed iron active sites, Energ. Environ. Sci. 12 (2019) 2548-2558.
- [37] J. Li, H. Zhang, W. Samarakoon, W. Shan, D.A. Cullen, S. Karakalos, M. Chen, D. Gu, K.L. More, G. Wang, Z. Feng, Z. Wang, G. Wu, Thermally driven structure and performance evolution of atomically dispersed FeN<sub>4</sub> sites for oxygen reduction, Angew. Chem. Int. Ed. 58 (2019) 18971-18980.
- [38] Q. Liu, X. Liu, L. Zheng, J. Shui, The solid-phase synthesis of an Fe-N-C electrocatalyst for high-power proton-exchange membrane fuel cells, Angew. Chem. Int. Edit. 57 (2017) 1204-1208.
- [39] D.N. Dybtsev, H. Chun, K. Kim, Rigid and flexible: A highly porous metal—organic framework with unusual guest-dependent dynamic behavior, Angew. Chem. Int. Ed. 43 (2004) 5033-5036.
- [40] W. Xia, J. Zhu, W. Guo, L. An, D. Xia, R. Zou, Well-defined carbon polyhedrons prepared from nano metal—organic frameworks for oxygen reduction, J. Mater. Chem. A 2 (2014) 11606-11613.
- [41] S. Zhao, H. Yin, L. Du, L. He, K. Zhao, L. Chang, G. Yin, H. Zhao, S. Liu, Z. Tang, Carbonized nanoscale metal—organic frameworks as high performance electrocatalyst for oxygen reduction reaction, ACS Nano 8 (2014) 12660-12668.
- [42] L. Jiao, G. Wan, R. Zhang, H. Zhou, S.-H. Yu, H.-L. Jiang, From metal-organic frameworks to single-atom Fe implanted N-doped porous carbons: efficient oxygen reduction in both alkaline and acidic media, Angew. Chem. Int. Ed. 57 (2018) 8525-8529.
- [43] F. Li, G.-F. Han, H.-J. Noh, S.-J. Kim, Y. Lu, H.Y. Jeong, Z. Fu, J.-B. Baek, Boosting oxygen reduction catalysis with abundant copper single atom active sites, Energy Environ. Sci. 11 (2018) 2263-2269.
- [44] P. Zhang, F. Sun, Z. Xiang, Z. Shen, J. Yun, D. Cao, ZIF-derived in situ nitrogen-doped porous carbons as efficient metal-free electrocatalysts for oxygen reduction reaction, Energy Environ. Sci. 7 (2014) 442-450.

- [45] R.V. Jagadeesh, K. Murugesan, A.S. Alshammari, H. Neumann, M.-M. Pohl, J. Radnik, M. Beller, MOF-derived cobalt nanoparticles catalyze a general synthesis of amines, Science 358 (2017) 326-332.
- [46] D.E. Nixon, G.S. Parry, A.R.J.P. Ubbelohde, Order-disorder transformations in graphite nitrates, Proc. R. Soc. Lond. A 291 (1966) 324–339.
- [47] Y. Holade, C. Morais, K. Servat, T.W. Napporn, K.B. Kokoh, Enhancing the available specific surface area of carbon supports to boost the electroactivity of nanostructured Pt catalysts, Phys. Chem. Chem. Phys. 16 (2014) 25609-25620.
- [48] Y. He, S. Liu, C. Priest, Q. Shi, G. Wu, Atomically dispersed metal-nitrogen-carbon catalysts for fuel cells: advances in catalyst design, electrode performance, and durability improvement, Chem. Soc. Rev. 49 (2020) 3484-3524.
- [49] S. Treimer, A. Tang, D.C. Johnson, A consideration of the application of Koutecký-Levich plots in the diagnoses of charge-transfer mechanisms at rotated disk electrodes, Electroanalysis 14 (2002) 165-171.
- [50] M.-H. Pham, G.-T. Vuong, F.d.r.-G. Fontaine, T.-O. Do, Rational synthesis of metalorganic framework nanocubes and nanosheets using selective modulators and their morphology-dependent gas-sorption properties, Cryst. Growth Des. 12 (2012) 3091-3095.
- [51] Z. Zhang, J. Sun, F. Wang, L. Dai, Efficient oxygen reduction reaction (ORR) catalysts based on single iron atoms dispersed on a hierarchically structured porous carbon framework, Angew. Chem. 130 (2018) 9176-9181.
- [52] Q. Liu, X. Liu, L. Zheng, J. Shui, The solid-phase synthesis of an Fe-N-C electrocatalyst for high-power proton-exchange membrane fuel cells, Angew. Chem. 130 (2018) 1218-1222.
- [53] D. Guo, R. Shibuya, C. Akiba, S. Saji, T. Kondo, J. Nakamura, Active sites of nitrogen-doped carbon materials for oxygen reduction reaction clarified using model catalysts, Science 351 (2016) 361-365.
- [54] E.H. Martins Ferreira, M.V.O. Moutinho, F. Stavale, M.M. Lucchese, R.B. Capaz, C.A. Achete, A. Jorio, Evolution of the Raman spectra from single-, few-, and many-layer graphene with increasing disorder, Phys. Rev. B 82 (2010) 125429.
- [55] M.S. Dresselhaus, A. Jorio, M. Hofmann, G. Dresselhaus, R. Saito, Perspectives on carbon nanotubes and graphene raman spectroscopy, Nano Lett. 10 (2010) 751-758.
- [56] R. Saito, M. Hofmann, G. Dresselhaus, A. Jorio, M.S. Dresselhaus, Raman spectroscopy of graphene and carbon nanotubes, Adv. Phys. 60 (2011) 413-550.

[57] P. Yan, B. Zhang, K.-H. Wu, D. Su, W. Qi, Surface chemistry of nanocarbon: Characterization strategies from the viewpoint of catalysis and energy conversion, Carbon 143 (2019) 915-936.

# **Graphical Abstract**





framework materials.

Yu Zhou received his B.S. degree from Taiyuan University of Technology in 2015. He then joined Tianjin University to pursue his Ph.D under the supervision of Professor Yuxin Wang. He joined Professor Hong Yang's group at the University of Illinois at Urbana-Champaign in 2018 as a joint PhD student. His research interests are the design and characterization of non-precious metal electrocatalysts for fuel cells based on metal-organic



oxygen reduction reaction.

A Chicago-native Talha went on to receive his B.S. in chemical engineering from the University of Illinois at Chicago in 2016. He immediately joined Professor Hong Yang's group at the University of Illinois at Urbana-Champaign. His thesis research has focused on the development and characterization of non-precious metal electrocatalysts for fuel cell applications. Specifically, he has worked on metal-organic framework materials and their utilization as precursors to catalytic materials for the



Yanling Ma received her B.S. at University of Science and Technology of Beijing in 2015. She then went to Shanghai Jiao Tong University to pursue her Ph.D under the supervision of Professor Jianbo Wu and Professor Tao Deng in the School of Materials Science and Engineering. She joined Professor Hong Yang's group at the University of Illinois at Urbana-Champaign in 2018 as a visiting scholar. Her doctoral research has focused on the design

and characterization of electrocatalysts for fuel cells and in situ TEM characterization of gas phase chemical reactions.



Haw-Wen Hsiao completed his Ph.D. in Materials Science and Engineering at University of Illinois Urbana-Champaign in 2021. After that, he worked in the same group as a postdoctoral researcher. His research focuses on developing novel transmission electron microscopy (TEM) techniques to quantitatively characterize defects and microstructures in structural materials.



Cheng Zhang graduated from Tsinghua University in 2017 with a Bachelor's Degree in chemical engineering. He then joined Professor Hong Yang's group in at the University of Illinois at Urbana-Champaign as a Ph.D student. His graduate research has focused on the development of cathode materials for energy storage devices and efficient electrocatalysts for oxygen evolution reaction.



Hong Yang is the Richard C. Alkire Chair in Chemical Engineering at UIUC. He received his PhD degree in 1998 from University of Toronto (with Geoffrey A. Ozin) and did his postdoctoral training as an NSERC Postdoctoral Fellow at Harvard University (with George M. Whitesides). He worked at University of Rochester between 2001 and 2011, moved to UIUC in 2012. He is an elected Fellow of AAAS, winner of the Doctoral Prize from NSERC Canada, and CAREER Award from US NSF. His research interests are on the material chemistry

approach to develop nanostructures for catalysis, energy, and sustainability applications.